

Targeted sequence capture array for phylogenetics and population genomics in the Salicaceae¹

3 Brian J. Sanderson^{2,3,6}, Stephen P. DiFazio³, Quentin C. Cronk⁴, Tao Ma⁵, Matthew S. Olson²

4 ²Department of Biological Sciences, Texas Tech University, Lubbock, TX 79409-3131 USA

5 ³Department of Biology, West Virginia University, Morgantown, WV, 26506 USA

6 ⁴Department of Botany, University of British Columbia, Vancouver, BC, V6T 1Z4 Canada

7 ⁵Key Laboratory of Bio-Resource and Eco-Environment of Ministry of Education, College of
8 Life Sciences, Sichuan University, Chengdu 610065, People's Republic of China

9

10 Email addresses: BJS: brian@biologicallyrelevant.com

11 SPD: spdifazio@mail.wvu.edu

12 QC: quentin.cronk@ubc.ca

13 TM: matao.yz@gmail.com

14 MSO: matt.olson@ttu.edu

15 ⁶Author for correspondence: brian@biologicallyrelevant.com

16

17 Number of words: 3831

18 ¹Manuscript received: _____; revision accepted _____.

19 **Abstract**

20 • **Premise of the study:** The family Salicaceae has proved taxonomically challenging,
21 especially in the genus *Salix*, which is speciose and features frequent hybridization and
22 polyploidy. Past efforts to reconstruct the phylogeny with molecular barcodes have failed to
23 resolve the species relationships of many sections of the genus.

24 • **Methods:** We used the wealth of sequence data in the family to design sequence capture
25 probes to target regions of 300-1200 base pairs of exonic regions of 972 genes.

26 • **Results:** We recovered sequence data for nearly all of the targeted genes in three species of
27 *Populus* and three species of *Salix*. We present a species tree, discuss concordance among
28 gene trees, as well as some population genomic summary statistics for these loci.

29 • **Conclusions:** Our sequence capture array has extremely high capture efficiency within the
30 genera *Populus* and *Salix*, resulting in abundant phylogenetic information. Additionally,
31 these loci show promise for population genomic studies.

32 **Key words:** Phylogenetics; *Populus*; Salicaceae; *Salix*; targeted sequence capture

33 **Introduction**

34 Although the cost of whole-genome sequencing has continued to dramatically decrease over the
35 past decade, the cost and complexity of whole-genome analyses still limit their utility and
36 accessibility for answering evolutionary questions in novel taxa (Richards, 2018). However, a
37 polished genome assembly is not necessary to address many questions. In this context, several
38 methods have been developed to reduce the cost and effort required to obtain genomic
39 information in novel species (McKain et al., 2018). The recent development of targeted sequence
40 capture presents an affordable method for consistently isolating specific, long, phylogenetically
41 informative regions in the taxa of interest (Gnirke et al., 2009; Mamanova et al., 2010; Hale et
42 al., 2020). Targeted sequence capture uses biotinylated RNA baits to target prepared sequencing
43 library fragments. The baited library fragments can then be pulled out of solution with
44 streptavidin-coated magnetic beads to selectively enrich the fragments that contain loci of
45 interest, while discarding the majority of library fragments that do not. This method offers many
46 advantages over other methods of genome sequence partitioning, such as genome skimming and
47 RAD-seq. It does not necessarily depend on a highly polished, annotated reference genome.
48 Additionally, the same loci can be consistently sequenced at a high depth across individuals
49 without requiring comprehensive, concurrent sequencing of all individuals (Mamanova et al.,
50 2010; Grover et al., 2012; Jones and Good, 2016).

51 In this paper, we report on the design and implementation of a targeted sequence capture
52 array to collect data for phylogenetic analysis within the Salicaceae, the plant family that
53 includes poplars and willows. Understanding species relationships within this family, and in
54 particular the genus *Salix*, has presented challenges to taxonomists as early as Linnaeus, who
55 noted that “species of this genus are extremely difficult to clarify” (Linnaeus, 1753; Skvortsov,

56 1999). *Salix* species present challenges to classification due to their wide geographic ranges,
57 hysteranthous phenology, extensive interspecific hybridization, polyploidy, and the lack of well-
58 defined and variable flower characters for morphological circumscription of taxa (Raup, 1959;
59 Skvortsov, 1999; Percy et al., 2014; Wang et al., 2020). Species of *Salix* exhibit holarctic
60 distributions, and there are several classifications which differ among continents and are
61 challenging to synthesize due to non-overlapping taxonomic treatment of species (Dickmann and
62 Kuzovkina, 2014). Past efforts to reconstruct the phylogeny of *Salix* using nuclear AFLP and
63 plastid barcode sequences have resulted in a lack of clearly resolved species relationships,
64 especially in the subgenus *Vetrix* (Trybush et al., 2008; Percy et al., 2014). A more recent study
65 using a supermatrix approach with RAD-seq data showed resolution within a subset of species of
66 the subgenera *Vetrix* and *Chamaetia*, highlighting the potential of large-scale molecular data to
67 resolve this phylogenetically challenging group (Wagner et al., 2018).

68 The utility of RAD-seq for collecting data for phylogeny, however, is limited by several
69 issues. First, RAD-seq does not consistently screen homologous regions across species and
70 across different experiments, which limits its utility for adding species to a phylogeny at a later
71 time. Second, because RAD-seq assesses diversity in very short segments of the genome, the
72 concatenation of this sort of data and supermatrix approaches are required for its use in
73 phylogenetic analyses requires (de Queiroz and Gatesy, 2007), which does not allow separate
74 exploration of gene and species phylogenies using super tree methods (Sanderson et al., 1998).
75 Additionally, concatenation approaches are likely to exacerbate problems associated with
76 maximum-likelihood methods for species with rapid diversification (Edwards et al., 2007;
77 Edwards, 2009). Targeted sequence capture does not have these limitations, and thus may be a
78 more appropriate genotyping platform for phylogenetics.

79 Species of *Populus* and *Salix* have been of great interest for the development of forestry
80 and biofuel products, resulting in polished reference genomes for *P. trichocarpa*, *P. tremula*, *P.*
81 *euphratica*, *S. purpurea* and *S. suchowensis*., as well as shallow resequencing data for many
82 additional species (Tuskan et al., 2018). Our design strategy leveraged this abundance of existing
83 genomic information to quantify polymorphism and the distribution of insertion- deletion events
84 within and among species in order to maximize capture efficiency. Additionally, because we
85 consistently target regions of exons we are able to characterize the nucleotide-site degeneracy
86 with these data to quantify population genomic summary statistics. We demonstrate the utility of
87 this resource for *Populus* and *Salix* species by presenting a fully resolved phylogenetic tree for
88 six species and an outgroup, and by estimating the distribution of nucleotide diversity within
89 species for our targeted genes.

90 **Methods**

91 *Probe Design*

92 Our goal was to identify regions that could be efficiently captured using RNA bait hybridization
93 for diverse species across the family Salicaceae. The family Salicaceae is thought to have
94 diverged from other clades approximately 92.5 Mya (Zhang et al., 2018b). Our primary focus
95 was on the genera *Populus* and *Salix*, which diverged approximately 48 Mya, and the species
96 *Idesia polycarpa* Maxim, which diverged from other clades approximately 56 Mya, which we
97 use as an outgroup (Zhang et al., 2018b). Although we were interested in using these probes for
98 phylogenetics with both *Populus* and *Salix* species, we focused on maximizing capture efficiency
99 for the species in *Salix*, because the phylogeny for *Populus* is already much better resolved than
100 that for *Salix* (Trybush et al., 2008; Wang et al., 2014, 2020; Percy et al., 2014; Liu et al., 2017).
101 For this reason, the capture baits were designed to target regions in *Salix pupurea* that also would

102 have high capture efficiency across the Salicaceae. The efficiency of RNA bait binding, and thus
103 capture efficiency, is reduced as target regions diverge due to sequence polymorphism (Lemmon
104 and Lemmon, 2013). To improve capture efficiency, we quantified sequence polymorphism
105 among whole-genome resequencing data from a diverse array of *Populus* and *Salix* species
106 (Table S1). The whole-genome short reads of the *Populus* and *Salix* species were aligned to the
107 *Populus trichocarpa* genome assembly version 3 (Tuskan et al., 2006) using bwa mem v. 0.7.12
108 with default parameters (Li, 2013). We used the *P. trichocarpa* genome as our initial reference
109 because it was the most polished and annotated genome in genus. Variable sites and insertion-
110 deletion mutations (indels) were identified using samtools mpileup (Li, 2011), and read depth for
111 the variant calls was quantified using vcftools (Danecek et al., 2011). Custom Python scripts
112 were used to identify variant and indel frequencies for all exons in the *P. trichocarpa* genome
113 annotation (scripts available at <https://github.com/BrianSanderson/phylo-seq-cap>; Sanderson,
114 2020).

115 Orthologs for our candidate loci in the in the *Salix purpurea* 94006 genome assembly
116 version 1 (*Salix purpurea* v1.0, DOE-JGI; Carlson et al., 2017; Zhou et al., 2018) were identified
117 using a list of orthologs between the *P. trichocarpa* and *S. purpurea* prepared using a tree-based
118 approach by Phytozome v 12 (Goodstein et al., 2012). We further screened candidate regions to
119 exclude high-similarity duplicated regions by accepting only loci with single BLAST (Camacho
120 et al., 2009) hits against the highly contiguous assembly of *S. purpurea* 94006 version 5 (Zhou et
121 al., 2020), which is less fragmented than the *S. purpurea* 94006 version 1. Genes from the
122 Salicoid whole-genome duplication were identified using MCScanX (Wang et al., 2012), using
123 default parameters and selected those segments for which the average K_S value for paralogous
124 genes was between 0.2 and 0.8. Genes for which at least 600 base pairs (bp) of exon sequence

125 contained 2-12% polymorphism and fewer than two indels were selected for probe design by
126 Arbor Biosciences (Ann Arbor, MI, USA). Probes were designed with 50% overlap across the
127 targeted regions, so that each nucleotide position would potentially be captured by two probes.
128 Finally, to ensure that loci with high divergence across the family would be captured, we
129 identified targets with less than 95% identity (based on BLAST results) between *S. purpurea* and
130 *P. trichocarpa* and designed supplementary probes from orthologs of these genes in the *Idesia*
131 *polycarpa* genome.

132 *Library Preparation and Sequence Capture*

133 Libraries for two individuals from each *Populus balsamifera* L., *P. tremula* L., *P. mexicana*
134 Wesmael., *Salix nigra* Marshall, *S. exigua* Nutt., and *S. phlebophylla* Andersson (Table S3) were
135 prepared using the NEBNext Ultra II DNA Prep Kit following the published protocol for this kit
136 (New England Biolabs, Ipswich, MA, USA), and quantified using an Agilent Bioanalyzer 2100
137 DNA 1000 kit (Agilent Technologies, Santa Clara, CA, USA). Libraries were pooled at
138 equimolar concentrations into two pools of six prior to probe hybridization following the Arbor
139 Biosciences myBaits protocol v 3.0.1 and Hale et al. (2020). The hybridized samples were
140 subsequently pooled at equimolar ratios and sequenced at the Texas Tech Center for
141 Biotechnology and Genomics using a MiSeq with the Micro chemistry and 150 bp paired-end
142 reads (Illumina, Inc., San Diego, CA, USA).

143 *Analysis of Sequence Capture Data*

144 Read data was trimmed for primer sequences and low quality scores using Trimmomatic v. 0.36
145 (Bolger et al., 2014). The trimmed read data, as well as the whole-genome reads for *I. polycarpa*,
146 were assembled into gene sequences using the HybPiper pipeline (Johnson et al., 2016). We
147 estimated the depth of read coverage across all targeted genes as well as at off-target sites in R.

148 The assembled amino acid sequences were aligned with mafft v. 7.310 with the parameters –
149 localpair and –maxiterate 1000 (Katoh and Standley, 2013), converted into codon-aligned
150 nucleotide alignments with pal2nal v. 14 (Suyama et al., 2006), and trimmed for quality and
151 large gaps with trimal v. 1.4.rev15 with the parameter -gt 0.5 (Capella-Gutiérrez et al., 2009).

152 HybPiper provides warnings for genes that have multiple competing assemblies that are
153 within 80% of the length of the target region, because the alternate alignments may indicate that
154 those genes have paralogous copies in the genome. We estimated phylogenetic relationships
155 using the full set of gene sequences recovered from our sequence capture data, as well as a
156 restricted set of putatively single copy genes, based on our *a priori* list of paralogs between *S.*
157 *purpurea* and *P. tricocarpa*, and supplemented by the list of paralog warnings from HybPiper.

158 We estimated gene trees using RAxML v. 8.2.10, specifying a GTR Γ model of sequence
159 evolution (Stamatakis, 2014). A set of 250 bootstrap replicates was generated for each gene tree.
160 We used ASTRAL-III to infer the species tree from the RAxML gene trees (Zhang et al., 2018a;
161 Rabiee et al., 2019). Because all nodes are weighted equally during quartet decomposition in
162 ASTRAL-III, we used sumtrees in the Python package DendroPy v. 4.4.0 to collapse nodes with
163 less than 33% bootstrap support values prior to species tree estimation (Sukumaran and Holder,
164 2010). A set of 100 multilocus bootstrap replicates was generated for the species tree. We used
165 phyparts to determine the extent of congruence among gene trees for each node in the species
166 tree (Smith et al., 2015). Cladograms representing the gene tree congruence and alternate
167 topologies were plotted with the scripts phypartspiecharts.py and minority_report.py, written by
168 Matt Johnson (scripts available at <https://github.com/mossmatters/phyloscripts>).

169 Finally, we used custom Python scripts to quantify nucleotide diversity at synonymous
170 and non-synonymous sites between the individuals of the same species, as well as correlations in

171 values of per-site nucleotide diversity between all species. The scripts described above as well as
172 the full details of these analyses including are available in Jupyter notebooks at
173 <https://github.com/BrianSanderson/phylo-seq-cap> (Sanderson, 2020).

174 **Results**

175 *Sequence capture efficiency*

176 The final capture kit targets 972 genes covered by 12,951 probes based on the *S. purpurea*
177 reference, and an additional 7049 (redundant) probes based on the *I. polycarpa* genome that
178 target genes with the highest divergence between *S. purpurea* and *P. trichocarpa* identified by
179 Phytozome. This included an average of 680 ± 309 (mean \pm sd) probes on each *S. purpurea*
180 chromosome (Table S2), with an average of 1098 ± 489 (mean \pm sd) bp of exon sequence per
181 gene. Of the 972 target genes, 593 are putatively single copy based on our identification of
182 paralogs in the *S. purpurea* genome assembly, 142 represent pairs of paralogs from the shared
183 Salicoid whole-genome duplication (i.e. 71 pairs of genes), and 237 are genes that have known
184 paralogs for which we were not able to design targets in this kit (i.e. each of these genes has one
185 or more paralogs in the *S. purpurea* genome that is not targeted by probes). We included a total
186 of 1219 genes in the target file used to assemble the capture data, which includes the 972
187 targeted genes as well as paralogous copies for which probes were not designed. Because the
188 issues of paralogy become more complex when we add species other than *S. purpurea* and *P.*
189 *trichocarpa*, we advise using the HybPiper warnings of multiple competing long assemblies to
190 assess paralogy in novel species following guidance here
191 <https://github.com/mossmatters/HybPiper/wiki/Paralogs>. The sequences of the capture probes as
192 well as the target reference file are accessible at <https://github.com/BrianSanderson/phylo-seq->

193 cap (Sanderson, 2020). The sequence capture kit is available from Arbor Biosciences
194 (Ref#170424-30 “Salicaceae”).

195 Sequence capture efficiency was high among the libraries. We recovered 805,820 ±
196 178,482 reads (mean ± sd) from our *Populus* and *Salix* target capture libraries, of which 86.7 ±
197 1.15% (mean ± sd) mapped to the target sequence reference (Table 1). An average of 94.48 ±
198 1.37% of targeted exon sequences were covered by \geq 10 reads. The average read depth was
199 44.65 ± 1.61 for on-target sites, and 14.48 ± 2.10 for off-target sites (Table S4).

200 *Phylogenetics*

201 The species tree estimated with putatively single copy genes correctly paired all individuals of
202 the same species and revealed a fully resolved phylogeny for the *Populus* and *Salix* species with
203 100% multilocus bootstrap support for all nodes (Fig. 1A). At least 85% of gene trees support the
204 topology of the species tree (Fig. 1B), with the exceptions of the bipartition that separates *P.*
205 *balsamifera* and *P. tremula*, and the bipartition that separates *S. phlebophylla* from the other
206 *Salix* species, which had dominant alternate topologies that were supported by a large number of
207 gene trees (Figs. S1 and S2). The topology of the species tree estimated with the full set of genes
208 and known paralogs was nearly identical to the tree estimated with only the putatively single
209 copy genes. The major difference between these trees was evident in the bipartition separating *P.*
210 *balsamifera* and *P. tremula*, where there were a large number of alternative topologies supported
211 by small numbers of gene trees (the top 3 were supported by 13, 11, and 10 gene trees; Fig. S3).

212 *Population genomics*

213 Patterns of nucleotide diversity, measured as Nei’s π (Nei and Li, 1979), varied among species,
214 with the greatest variation at synonymous sites (Fig. S4; Table S5). *P. tremula* had the highest
215 average values of π at both synonymous and non-synonymous sites (Fig. 2). The values of π

216 among species were highly correlated for species within genus and exhibited lower correlations
217 between genera (Fig. 3).

218 **Discussion**

219 The decreasing cost of obtaining genomic and transcriptomic sequence data holds great promise
220 for unlocking our understanding of phylogenetic relationships and population genetic patterns
221 within and among complex taxonomic groups. However, assembling complete genomes is still
222 not a trivial task, and there exist relatively few polished plant reference genomes onto which
223 genome skimming data can be mapped. Many methods have been developed to reduce the
224 sequencing and analytical burdens associated with obtaining genome data. We believe that
225 targeted sequence capture is one of the most promising contemporary methods of inexpensively
226 generating genomic information.

227 The efficiency of our targeted sequence capture array was extremely high, which yielded
228 abundant phylogenetic information for six species of *Populus* and *Salix*. Overall, the phylogeny
229 was fully resolved and conformed to our general understanding the relationships among the taxa
230 (Wu et al., 2015; Wang et al., 2020). One strength of the sequence capture approach is that it
231 provides sufficiently long contiguous segments of gene sequences to assemble gene trees and it
232 can overcome the problems introduced by concatenation of multiple gene regions with divergent
233 histories (Edwards et al., 2007; Edwards, 2009). The super tree approach also allowed for the
234 identification of alternative evolutionary histories that are supported by different regions of the
235 genome, as often occurs during historical hybridization and introgression (Zhang et al., 2018a;
236 Rabiee et al., 2019). Our species tree identified three alternative gene tree relationships among
237 the three *Populus* species (Fig. S1). Previous studies have provided evidence of historical
238 introgression among these species, including a history of chloroplast capture and hybridization

239 between *P. mexicana* and species in the section *Tacamahaca* (including *P. balsamifera*; Wang et
240 al., 2014, 2020; Liu et al., 2017). The second most supported alternative topology that we
241 recovered placed *P. mexicana* and *P. tremula* as sister taxa, a pattern that does not support this
242 hypothesis, likely due to incomplete lineage sorting (Wang et al., 2020). *P. tremula* likely has a
243 greater long-term effective population size than *P. balsamifera* (Wang et al., 2016), and so
244 coalescence times may be shorter on average in *P. balsamifera*. Among the *Salix* species, we
245 identified three alternative gene tree relationships between the *S. phlebophylla* and *S. exigua*
246 individuals, which may reflect the histories of rapid speciation and hybridization that have long
247 vexed attempts at phylogenetic reconstruction in the genus *Salix* (Fig. S2; Trybush et al., 2008;
248 Percy et al., 2014). Both of these patterns in *Populus* and *Salix* may be better understood once
249 additional taxa are added to this phylogeny.

250 We have also shown that this sequence capture design can be applied to address questions
251 related to population genomics in the Salicaceae. Many of the advantages of targeted sequence
252 capture over competing methods are of particular relevance for population genomics studies,
253 including specific knowledge of loci being sequenced, the ability to differentiate among
254 synonymous, non-synonymous, intronic, and intergenic loci, and the ability to collect data on the
255 same set of loci across different experiments, either within species or across species, for
256 comparative studies. In particular, synonymous sites, especially four-fold synonymous sites, are
257 among the fastest evolving regions of the genome and the sites within genic regions least
258 influenced by selection (Wright and Andolfatto, 2008), and are thus among the best regions for
259 estimating patterns of historical demography. Our estimates of nucleotide diversity are similar to
260 those that have been previously reported for *P. balsamifera* and *P. tremula* using Sanger
261 sequencing data (Ingvarsson, 2005; Olson et al., 2010) and whole-genome sequencing data

262 (Wang et al., 2016). The high estimates of diversity in *S. phlebophylla* compared to the other two
263 *Salix* species is curious and may result from a history with relatively little migration due to the
264 absence of glaciation over a large portion of its Beringian distribution (Hultén, 1937).

265 The current study is based on a small sample size per species (n = 2), and so our ability to
266 account for population structure or robustly perform population genomic inferences with these
267 data is limited. Additionally, a potential limitation for using this sequence capture array for
268 comparative population genomics is that we screened loci for a range of among-species
269 variability between 2-12%, which excludes loci that exhibit extremely high or low values of
270 nucleotide diversity. This may bias estimates of nucleotide diversity arising from these probes
271 toward greater evenness. The ability to identify synonymous sites, which are the closest to
272 neutral among all classes of sites (Wright and Andolfatto, 2008), should partially address this
273 bias. Another feature of sequence capture data is the recovery of “off-target” sequences that
274 result from the fact that the insert size of libraries is larger than the 120 bp bait length, and so
275 regions upstream and downstream of the target will be sequenced as well. These regions may
276 include intronic and intergenic regions, as well as exonic sequences that deviate from the
277 constraints we used for our design. The results we report here only incorporate the “on-target”
278 sites that we sequenced, but HybPiper implements methods to assemble intronic sequences as
279 well. However, the potential effects of hitchhiking selection on synonymous site variation will
280 likely remain apparent.

281 We also found that it was straightforward to integrate the targeted sequence capture data
282 with whole-genome sequence data using the HybPiper pipeline by simply including the FASTQ
283 files from whole-genome reads in the pipeline. This strategy was used to successfully incorporate
284 whole-genome sequencing data from *Idesia polycarpa*, to act as our outgroup. The proportion of

285 gene coverage as well as the read depth for the *I. polycarpa* data was similar to the sequence
286 capture libraries (Table 1).

287 A whole genome duplication occurred prior to the divergence of *Salix* and *Populus*, and
288 there are at least 8000 known paralog pairs in the *P. trichocarpa* reference genome (Tuskan et
289 al., 2006). Genes with paralogous copies in the genome can complicate gene assemblies, because
290 sequence data from both copies may alternately align to the same target sequence. We identified
291 paralogous sequences in the *S. purpurea* genome assembly using MCScanX, and used that
292 information to assist in the design the sequence capture array. The final array includes 593
293 putatively single copy genes, 142 pairs of paralogs, and 237 genes which have paralogs but for
294 which we were not able to include both paralogs in the kit due our selection criteria. The target
295 reference file we used to map the sequence capture data thus includes 1219 genes including the
296 single copy and known paralogs from *S. purpurea*. In addition to this, HybPiper provides
297 warnings for genes that have multiple competing alignments that cover the majority of the target
298 sequence, which may indicate the presence of multiple paralogous copies in the genome
299 (Johnson et al., 2016). This will be particularly useful because the genes that have maintained
300 paralogous copies are likely to differ among species throughout the diversification of willows.
301 We estimated evolutionary relationships using both the full set of 1219 single copy and known
302 paralog genes, as well as a limited set of just single copy genes that did not report paralog
303 warnings. The results from both analyses were nearly the same, but this will likely not be true for
304 a more complex phylogenetic analysis that includes more than six species and an outgroup. For
305 those more complex phylogenetic analyses, the ability to compare trees constructed with single
306 copy genes with those using paralogous copies may provide crucial information for reconciling
307 evolutionary relationships.

308 This sequence capture array will provide the community with an excellent resource to
309 consistently sequence a set of variable regions of the genome for phylogenetic and population
310 genomic investigations in the Salicaceae. The rate of read mapping and coverage of target genes
311 was remarkably consistent across both genera, despite the fact that the taxa were selected to
312 maximize sampling of phylogenetic diversity within each genus. The Salicaceae are important
313 plants in the northern hemisphere both ecologically and economically and have been the subjects
314 of numerous population genetics and genomics investigations of speciation, hybridization,
315 introgression, selection, and historical population size and migration. This resource will allow
316 phylogenetic and comparative population genomic studies to assess the same loci across different
317 studies, which will allow us to build a worldwide diversity database and facilitate more precise
318 comparative research questions. Our results demonstrate that the rate of gene capture is
319 extremely high, such that it would be unnecessary to filter data and determine appropriate
320 overlapping genotype thresholds, as is necessary with random genome partitioning methods such
321 as RAD-seq.

322 **Acknowledgements**

323 We thank M. Johnson for help with data analysis, P. Ingvarsson for help collecting *Populus*
324 *tremula*, and J. Martinez, Instituto de Geología, UNAM, Hermosillo, Mexico for help collecting
325 *Populus mexicana*. We thank J. Phillips for his work at Phytozome in identifying orthologs
326 between *P. trichocarpa* and *S. purpurea*. Funding for this project was provided by the US
327 National Science Foundation (1542509 and 1542599), Genome Canada (168BIO), and the
328 National Natural Science Foundation of China (31561123001). The genetic material used to
329 generate the genomic resources from AgCanBaP (Agriculture Canada Balsam Poplar) collection
330 belong to Her Majesty the Queen in Right of Canada as represented by the Minister of

331 Agriculture and Agri-Food. Agriculture and Agri-Food Canada retains complete ownership of
332 the resources presented here.

333 **Author Contributions**

334 S.P.D. and M.S.O. conceived the study. S.P.D., Q.C.C., T.M., and M.S.O. secured funding to
335 support the project. B.J.S. and S.P.D. designed the sequence capture array. Q.C.C. and T.M.
336 provided whole genome sequence data. B.J.S and M.S.O. prepared and sequenced the DNA
337 samples, analyzed the data, interpreted the results, and wrote the manuscript. All authors edited
338 drafts of the manuscript.

339 **Data Accessibility**

340 Accession numbers for all sequence data used to design the sequence capture array are presented
341 in Table S1. The raw reads of targeted sequence capture data from the six species of *Populus* and
342 *Salix* are available on the NCBI sequence read archive under the BioProject accession number
343 PRJNA627181. The raw reads of the *Idesia polycarpa* whole genome sequence data are available
344 in the Genome Warehouse of the Beijing Institute of Genomics (BIG), under the accession
345 number PRJCA002959. The sequences of the probes that were designed, all of the custom
346 Python scripts that were used for this study, and the full details of analyses summarized in
347 notebooks are available at <https://github.com/BrianSanderson/phylo-seq-cap> (Sanderson, 2020).

348 **Literature Cited**

349 BOLGER, A.M., M. LOHSE, and B. USADEL. 2014. Trimmomatic: A flexible trimmer for Illumina
350 sequence data. *Bioinformatics* 30: 2114–2120.

351 CAMACHO, C., G. COULOURIS, V. AVAGYAN, N. MA, J. PAPADOPoulos, K. BEALER, and T.L.
352 MADDEN. 2009. BLAST+: Architecture and applications. *BMC Bioinformatics* 10: 421–421.

353 CAPELLA-GUTIÉRREZ, S., J.M. SILLA-MARTÍNEZ, and T. GABALDÓN. 2009. trimAl: A tool for
354 automated alignment trimming in large-scale phylogenetic analyses. *Bioinformatics* 25: 1972–
355 1973.

356 CARLSON, C.H., Y. CHOI, A.P. CHAN, M.J. SERAPIGLIA, C.D. TOWN, and L.B. SMART. 2017.
357 Dominance and Sexual Dimorphism Pervade the *Salix purpurea* L. Transcriptome. *Genome*
358 *Biology and Evolution* 9: 2377–2394.

359 DANECEK, P., A. AUTON, G. ABECASIS, C.A. ALBERS, E. BANKS, M.A. DEPRISTO, R.E.
360 HANDSAKER, ET AL. 2011. The variant call format and VCFtools. *Bioinformatics* 27: 2156–2158.

361 DE QUEIROZ, A., and J. GATESY. 2007. The supermatrix approach to systematics. *Trends in*
362 *Ecology and Evolution* 22: 34–41.

363 DICKMANN, D.I., and J. KUZOVKINA. 2014. Poplars and Willows of the World, With Emphasis
364 on Silviculturally Important Species. *In* J. Isebrands, and J. Richardson [eds.], *Poplars and*
365 *Willows Trees for Society and the Environment*, 8–91. The Food and Agriculture Organization
366 of the United Nations, Rome, Italy.

367 DOE-JGI. *Salix purpurea* version 1.

368 EDWARDS, S.V. 2009. Is a new and general theory of molecular systematics emerging? *Evolution*
369 63: 1–19.

370 EDWARDS, S.V., L. LIU, and D.K. PEARL. 2007. High-resolution species trees without
371 concatenation. *Proceedings of the National Academy of Sciences* 104: 5936–5941.

372 GNRKE, A., A. MELNIKOV, J.R. MAGUIRE, P. ROGOV, E.M. LEPROUST, W. BROCKMAN, T.J.

373 FENNELL, ET AL. 2009. Solution hybrid selection with ultra-long oligonucleotides for massively

374 parallel targeted sequencing. *Nature Biotechnology* 27: 182–189.

375 GOODSTEIN, D.M., S. SHU, R. HOWSON, R. NEUPANE, R.D. HAYES, J. FAZO, T. MITROS, ET AL.

376 2012. Phytozome: A comparative platform for green plant genomics. *Nucleic Acids Research* 40:

377 D1178–D1186.

378 GROVER, C.E., A. SALMON, and J.F. WENDEL. 2012. Targeted sequence capture as a powerful

379 tool for evolutionary analysis. *American Journal of Botany* 99: 312–319.

380 HALE, H., E.M. GARDNER, J. VIRUEL, L. POKORNY, and M.G. JOHNSON. 2020. Strategies for

381 reducing per-sample costs in target capture sequencing for phylogenomics and population

382 genomics in plants: Low-cost Hyb-Seq. *Applications in Plant Sciences* 11337.

383 HULTÉN, E. 1937. Outline of the history of arctic and boreal biota during the Quarternary period :

384 Their evolution during and after the glacial period as indicated by the equiformal progressive

385 areas of present plant species. Bokförlags aktiebolaget Thule, Stockholm, Sweden.

386 INGVARSSON, P.K. 2005. Nucleotide polymorphism and linkage disequilibrium within and

387 among natural populations of European aspen (*Populus tremula* L., Salicaceae). *Genetics* 169:

388 945–953.

389 JOHNSON, M.G., E.M. GARDNER, Y. LIU, R. MEDINA, B. GOFFINET, A.J. SHAW, N.J.C. ZEREGA,

390 and N.J. WICKETT. 2016. HybPiper: Extracting Coding Sequence and Introns for Phylogenetics

391 from High-Throughput Sequencing Reads Using Target Enrichment. *Applications in Plant*

392 *Sciences* 4: 1600016–1600016.

393 JONES, M.R., and J.M. GOOD. 2016. Targeted capture in evolutionary and ecological genomics.

394 *Molecular Ecology* 25: 185–202.

395 KATOH, K., and D.M. STANDLEY. 2013. MAFFT Multiple Sequence Alignment Software

396 Version 7: Improvements in Performance and Usability. *Molecular Biology and Evolution* 30:

397 772–780.

398 LEMMON, E.M., and A.R. LEMMON. 2013. High-Throughput Genomic Data in Systematics and

399 Phylogenetics. *Annual Review of Ecology, Evolution, and Systematics* 44: 99–121.

400 LI, H. 2013. Aligning sequence reads, clone sequences and assembly contigs with BWA-MEM.

401 00: 1–3.

402 LI, H. 2011. A statistical framework for SNP calling, mutation discovery, association mapping

403 and population genetical parameter estimation from sequencing data. *Bioinformatics* 27: 2987–

404 2993.

405 LINNAEUS, C. 1753. Species plantarum. Impensis Laurentii Salvii, Stockholm.

406 LIU, X., Z. WANG, W. SHAO, Z. YE, and J. ZHANG. 2017. Phylogenetic and Taxonomic Status

407 Analyses of the Abaso Section from Multiple Nuclear Genes and Plastid Fragments Reveal New

408 Insights into the North America Origin of *Populus* (Salicaceae). *Frontiers in Plant Science* 7: 1–

409 9.

410 MAMANOVA, L., A.J. COFFEY, C.E. SCOTT, I. KOZAREWA, E.H. TURNER, A. KUMAR, E. HOWARD,

411 ET AL. 2010. Target-enrichment strategies for next-generation sequencing. *Nature Methods* 7:

412 111–118.

413 MCKAIN, M.R., M.G. JOHNSON, S. URIBE-CONVERS, D. EATON, and Y. YANG. 2018. Practical
414 considerations for plant phylogenomics. *Applications in Plant Sciences* 6: e1038–e1038.

415 NEI, M., and W.H. LI. 1979. Mathematical model for studying genetic variation in terms of
416 restriction endonucleases. *Proceedings of the National Academy of Sciences* 76: 5269–5273.

417 OLSON, M.S., A.L. ROBERTSON, N. TAKEBAYASHI, S. SILIM, W.R. SCHROEDER, and P. TIFFIN.
418 2010. Nucleotide diversity and linkage disequilibrium in balsam poplar (*Populus balsamifera*).
419 *New Phytologist* 186: 526–536.

420 PERCY, D.M., G.W. ARGUS, Q.C. CRONK, A.J. FAZEKAS, P.R. KESANAKURTI, K.S. BURGESS,
421 B.C. HUSBAND, ET AL. 2014. Understanding the spectacular failure of DNA barcoding in willows
422 (*Salix*): Does this result from a trans-specific selective sweep? *Molecular Ecology* 23: 4737–
423 4756.

424 RABIEE, M., E. SAYYARI, and S. MIRARAB. 2019. Multi-allele species reconstruction using
425 ASTRAL. *Molecular Phylogenetics and Evolution* 130: 286–296.

426 RAUP, H.M. 1959. The willows of boreal Western America. *Contributions from the Gray*
427 *Herbarium of Harvard University* 185: 3–95.

428 RICHARDS, S. 2018. Full disclosure: Genome assembly is still hard. *PLOS Biology* 16:
429 e2005894–e2005894.

430 SANDERSON, B.J. 2020. BrianSanderson/phylo-seq-cap: Publication (Version v1.0). Zenodo.
431 <http://doi.org/10.5281/zenodo.3979562>.

432 SANDERSON, M.J., A. PURVIS, and C. HENZE. 1998. Phylogenetic supertrees: Assembling the
433 trees of life. *Trends in Ecology and Evolution* 13: 105–109.

434 SKVORTSOV, A.K. 1999. Willows of Russia and Adjacent Countries. I. N. (. Kadis, G. R. Argus,
435 and A. G. Zinovjev [eds.], University of Joensuu, Joensuu.

436 SMITH, S.A., M.J. MOORE, J.W. BROWN, and Y. YANG. 2015. Analysis of phylogenomic datasets
437 reveals conflict, concordance, and gene duplications with examples from animals and plants.
438 *BMC Evolutionary Biology* 15: 150–150.

439 STAMATAKIS, A. 2014. RAxML version 8: A tool for phylogenetic analysis and post-analysis of
440 large phylogenies. *Bioinformatics* 30: 1312–1313.

441 SUKUMARAN, J., and M.T. HOLDER. 2010. DendroPy: A Python library for phylogenetic
442 computing. *Bioinformatics* 26: 1569–1571.

443 SUYAMA, M., D. TORRENTS, and P. BORK. 2006. PAL2NAL: Robust conversion of protein
444 sequence alignments into the corresponding codon alignments. *Nucleic Acids Research* 34:
445 W609–W612.

446 TRYBUSH, S., Š. JAHODOVÁ, W. MACALPINE, and A. KARP. 2008. A genetic study of a *Salix*
447 germplasm resource reveals new insights into relationships among subgenera, sections, and
448 species. *Bioenergy Research* 1: 67–79.

449 TUSKAN, G.A., S.P. DIFAZIO, S. JANSSON, J. BOHLMANN, I. GRIGORIEV, U. HELLSTEN, N.
450 PUTNAM, ET AL. 2006. The Genome of Black Cottonwood, *Populus trichocarpa* (Torr. & Gray).
451 *Science* 313: 1596–1604.

452 TUSKAN, G.A., A.T. GROOVER, J. SCHMUTZ, S.P. DIFAZIO, A. MYBURG, D. GRATTAPAGLIA, L.B.

453 SMART, ET AL. 2018. Hardwood Tree Genomics: Unlocking Woody Plant Biology. *Frontiers in*

454 *Plant Science* 9: 1799–1799.

455 WAGNER, N.D., S. GRAMLICH, and E. HÖRANDL. 2018. RAD sequencing resolved phylogenetic

456 relationships in European shrub willows (*Salix* L. Subg. *Chamaetia* and subg. *Vetrix*) and

457 revealed multiple evolution of dwarf shrubs. *Ecology and Evolution* 8: 8243–8255.

458 WANG, J., N.R. STREET, D.G. SCOFIELD, and P.K. INGVARSSON. 2016. Natural Selection and

459 Recombination Rate Variation Shape Nucleotide Polymorphism Across the Genomes of Three

460 Related *Populus* Species. *Genetics* 202: 1185–1200.

461 WANG, M., L. ZHANG, Z. ZHANG, M. LI, D. WANG, X. ZHANG, Z. XI, ET AL. 2020.

462 Phylogenomics of the genus *Populus* reveals extensive interspecific gene flow and balancing

463 selection. *New Phytologist* 225: 1370–1382.

464 WANG, Y., H. TANG, J.D. DEBARRY, X. TAN, J. LI, X. WANG, T.-H. LEE, ET AL. 2012. MCScanX:

465 A toolkit for detection and evolutionary analysis of gene synteny and collinearity. *Nucleic Acids*

466 *Research* 40: e49–e49.

467 WANG, Z., S. DU, S. DAYANANDAN, D. WANG, Y. ZENG, and J. ZHANG. 2014. Phylogeny

468 reconstruction and hybrid analysis of *populus* (Salicaceae) based on nucleotide sequences of

469 multiple single-copy nuclear genes and plastid fragments. *PLoS ONE* 9:.

470 WRIGHT, S.I., and P. ANDOLFATTO. 2008. The Impact of Natural Selection on the Genome:

471 Emerging Patterns in *Drosophila* and *Arabidopsis*. *Annual Review of Ecology, Evolution, and*

472 *Systematics* 39: 193–213.

473 WU, J., T. NYMAN, D.-C. WANG, G.W. ARGUS, Y.-P. YANG, and J.-H. CHEN. 2015. Phylogeny of
474 *Salix* subgenus *Salix* s.l. (Salicaceae): Delimitation, biogeography, and reticulate evolution.
475 *BMC Evolutionary Biology* 15: 31.

476 ZHANG, C., M. RABIEE, E. SAYYARI, and S. MIRARAB. 2018a. ASTRAL-III: Polynomial time
477 species tree reconstruction from partially resolved gene trees. *BMC Bioinformatics* 19: 153–153.

478 ZHANG, L., Z. XI, M. WANG, X. GUO, and T. MA. 2018b. Plastome phylogeny and lineage
479 diversification of Salicaceae with focus on poplars and willows. *Ecology and Evolution* 8: 7817–
480 7823.

481 ZHOU, R., D. MACAYA-SANZ, C.H. CARLSON, J. SCHMUTZ, J.W. JENKINS, D. KUDRNA, A.
482 SHARMA, ET AL. 2020. A willow sex chromosome reveals convergent evolution of complex
483 palindromic repeats. *Genome Biology* 21: 38–38.

484 ZHOU, R., D. MACAYA-SANZ, E. RODGERS-MELNICK, C.H. CARLSON, F.E. GOUKER, L.M.
485 EVANS, J. SCHMUTZ, ET AL. 2018. Characterization of a large sex determination region in *Salix*
486 *purpurea* L. (Salicaceae). *Molecular Genetics and Genomics* 293: 1437–1452.

487

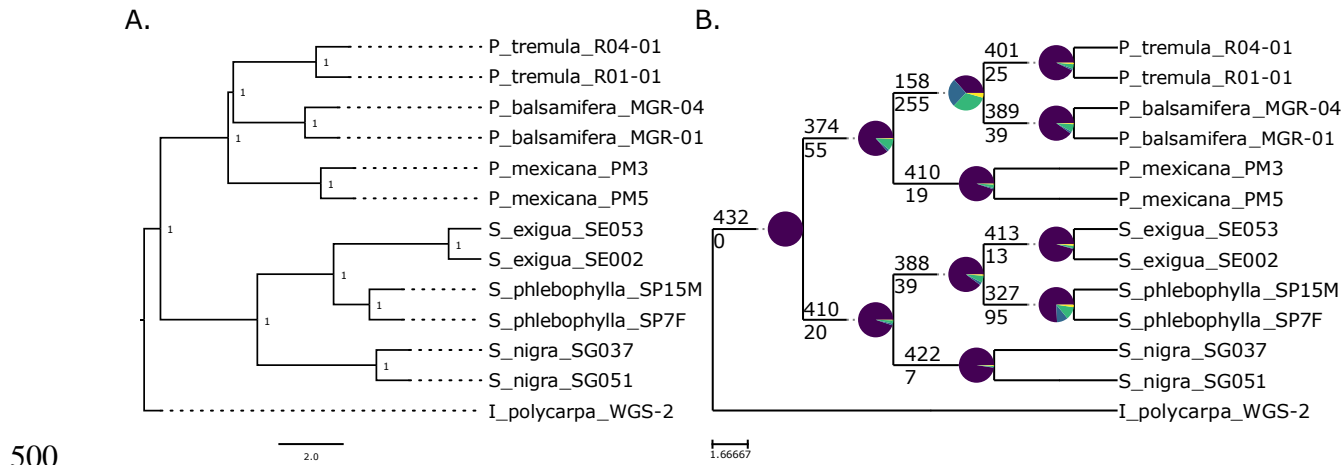
488 **Tables**

Name	Num. Reads	Reads Mapped	Prop. Mapped	Genes Mapped	Genes with 25% Seq	Genes with 50% Seq	Genes with 75% Seq	Genes with 100% Seq
L_polycarpa_WGS-2	223470714	1653494	0.007	971	970	966	944	123
P_balsamifera_MGR-01	614093	523321	0.852	972	971	960	884	122
P_balsamifera_MGR-04	769303	659712	0.858	972	972	965	915	145
P_mexicana_PM3	843032	739728	0.878	972	972	964	917	140
P_mexicana_PM5	880962	768927	0.873	972	972	967	913	142
P_tremula_R01-01	749220	638002	0.852	971	970	960	907	134
P_tremula_R04-01	634625	539805	0.851	971	969	956	876	122
S_exigua_SE002	1139616	998698	0.876	969	969	966	937	229
S_exigua_SE053	843120	741938	0.88	969	969	964	928	195
S_nigra SG037	1166615	1028635	0.882	971	971	967	932	205
S_nigra SG051	602649	524993	0.871	971	970	961	903	136
S_phlebophylla_SP15M	753628	651791	0.865	972	972	967	939	204
S_phlebophylla_SP7F	672975	581147	0.864	972	972	967	925	203

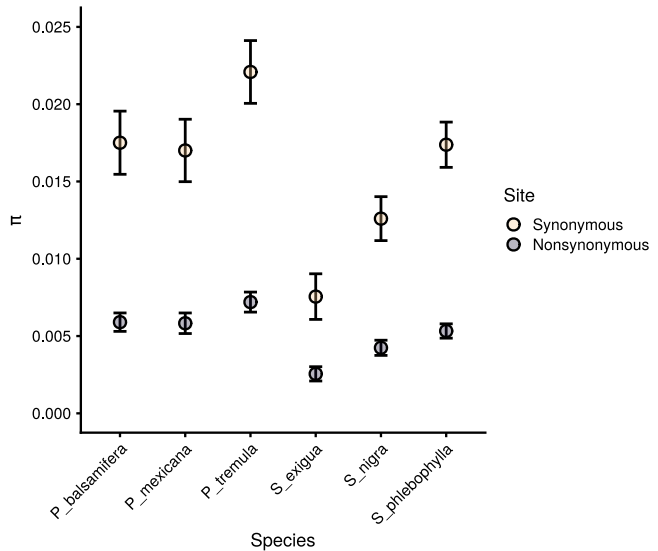
489

490 **Table 1.** Coverage summary statistics for sequence capture read data. For each library, values
491 represent the number of reads in the sequenced library, the number of those reads that mapped to
492 the reference file for the targeted genes, the proportion of mapped reads, the number of targeted
493 genes (out of 972) that had read data mapped to them, and the number of genes that had 25%,
494 50%, 75%, and 100% of the targeted sequences covered with > 10X reads. Footnote: the
495 L_polycarpa_WGS-2 data is from whole-genome sequencing data, rather than targeted sequence
496 capture, and thus the low percent of read mapping reflects the lack of target enrichment
497 (although the read coverage across targets was comparable to the sequence capture libraries,
498 Table S3).

499 **Figures**

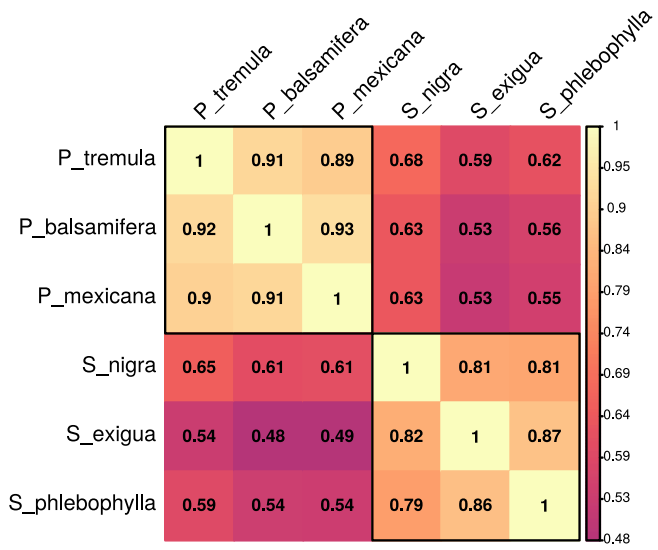


501 **Figure 1.** Species trees estimated for the 432 putatively single copy genes that did not have
502 paralog warnings reported by HybPiper. **A)** Species tree generated by ASTRAL-III for the gene
503 trees. Node values represent bootstrap support from 100 multilocus bootstrap replicates in
504 ASTRAL-III. Branch lengths represent coalescent units. **B)** Cladogram showing the congruence
505 of gene trees for all nodes in the ASTRAL-III species tree. The numbers above each node
506 represent the number of gene trees that support the displayed bipartition, and numbers below the
507 node represent the number of gene trees that support all alternate bipartitions. Purple wedges
508 represent the proportion of gene trees that support the displayed bipartition. Blue wedges
509 represent the proportion of gene trees that support a single alternative bipartition (see Figs S1 &
510 S2). Green wedges represent the proportion of gene trees that have multiple conflicting
511 bipartitions. Yellow wedges represent the proportion of gene trees that have no supported
512 bipartition. Plotting code and its interpretation were provided by Matt Johnson (for more detail,
513 see:
514 https://github.com/mossmatters/MJPythonNotebooks/blob/master/PhyParts_PieCharts.ipynb)



515

516 **Figure 2.** Means and 95% confidence intervals of values of nucleotide diversity (Nei's π) within
517 each species at synonymous (yellow) and nonsynonymous (purple) sites.



518

519 **Figure 3.** Pairwise correlation (Pearson's r) of values of Nei's π between all species. Values
520 above the diagonal represent the correlation of π at synonymous sites, values below the diagonal
521 represent non-synonymous sites. Black boxes represent within-genus comparisons.

522 **Supporting Information**

523 **Table S1.** Coverage summary statistics for whole-genome reads used to design sequence capture
524 array. For each library, values represent the name of the sequenced individual, the number of
525 reads in the sequenced library, the number of reads that mapped to the *Populus trichocarpa* v3
526 reference genome, the proportion of reads that mapped to the reference genome, and the mean
527 and standard deviation of read depth.

528 **Table S2.** Distribution of probes across the *Salix purpurea* genome.

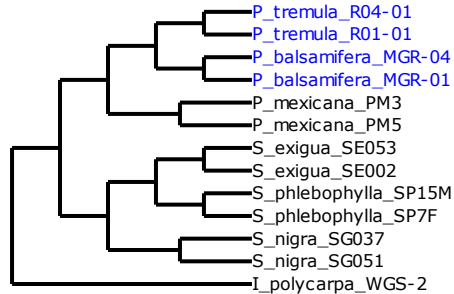
529 **Table S3.** Collection details for *Populus* and *Salix* species.

530 **Table S4.** Summary of read depth at on- and off-target sites. For each library values represent
531 the 5%, 25%, 50%, 75%, and 99% quantiles of read depth, the maximum number of reads
532 mapped to a site, and the mean and standard deviation of read depth.

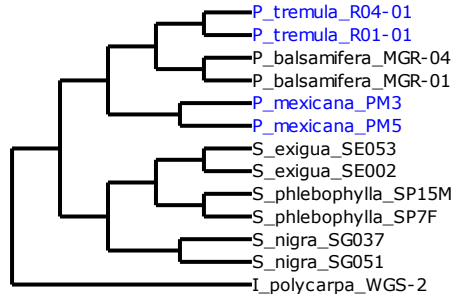
533 **Table S5.** Nucleotide diversity expressed as Nei's π for nonsynonymous and synonymous sites.

534 **Supplemental Figures**

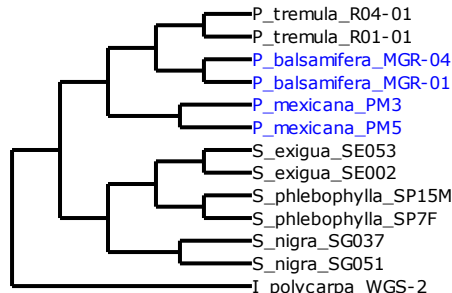
Most supported bipartition (158 gene trees)



Alternate bipartition (114 gene trees)



Alternate bipartition (94 gene trees)



535

536 **Figure S1.** Alternate bipartitions for the three species of *Populus*, based on gene tree

537 concordance. The cladogram in all three panels is that of the ASTRAL-III species tree (Figure

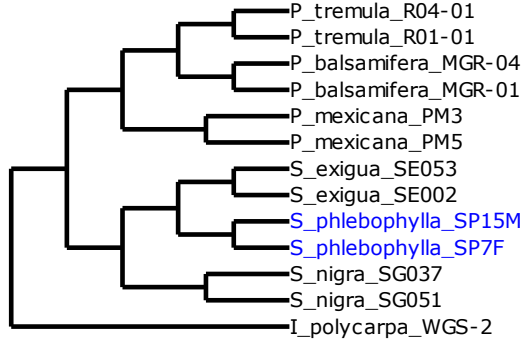
538 1), and the blue color represents the bipartition supported by the indicated number of gene trees

539 in each panel. **A)** 158 gene trees support the displayed ASTRAL-III species tree topology. **B)**

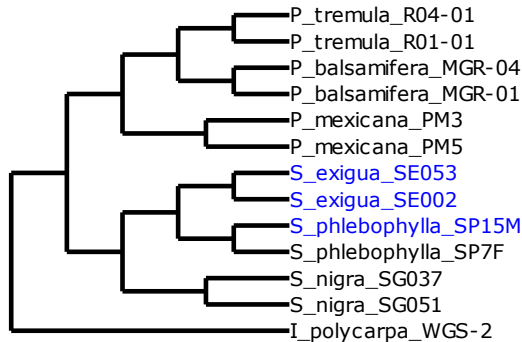
540 114 gene trees support a bipartition that places *P. tremula* and *P. mexicana* together. **C)** 94 gene

541 trees support a bipartition that places *P. balsamifera* and *P. mexicana* together.

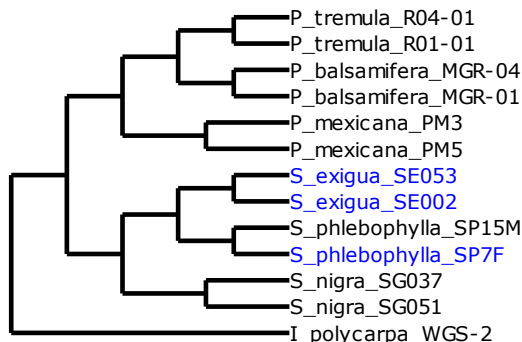
Most supported bipartition (327 gene trees)



Alternate bipartition (44 gene trees)



Alternate bipartition (39 gene trees)



542

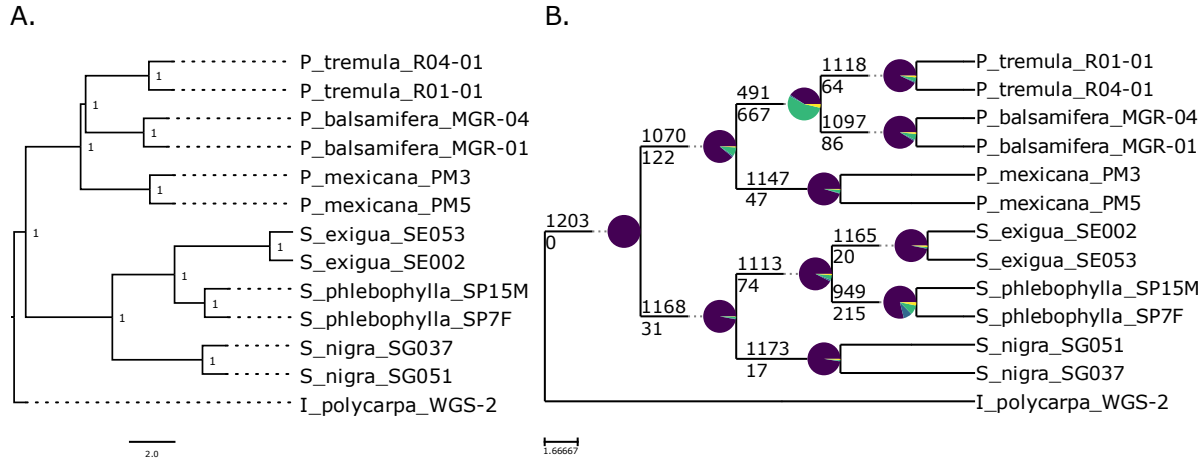
543 **Figure S2.** Alternate bipartitions for the three species of *Salix*, based on gene tree concordance.

544 The cladogram in all three panels is that of the ASTRAL-III species tree (Figure 1), and the blue

545 color represents the bipartition supported by the indicated number of gene trees in each panel. **A)**

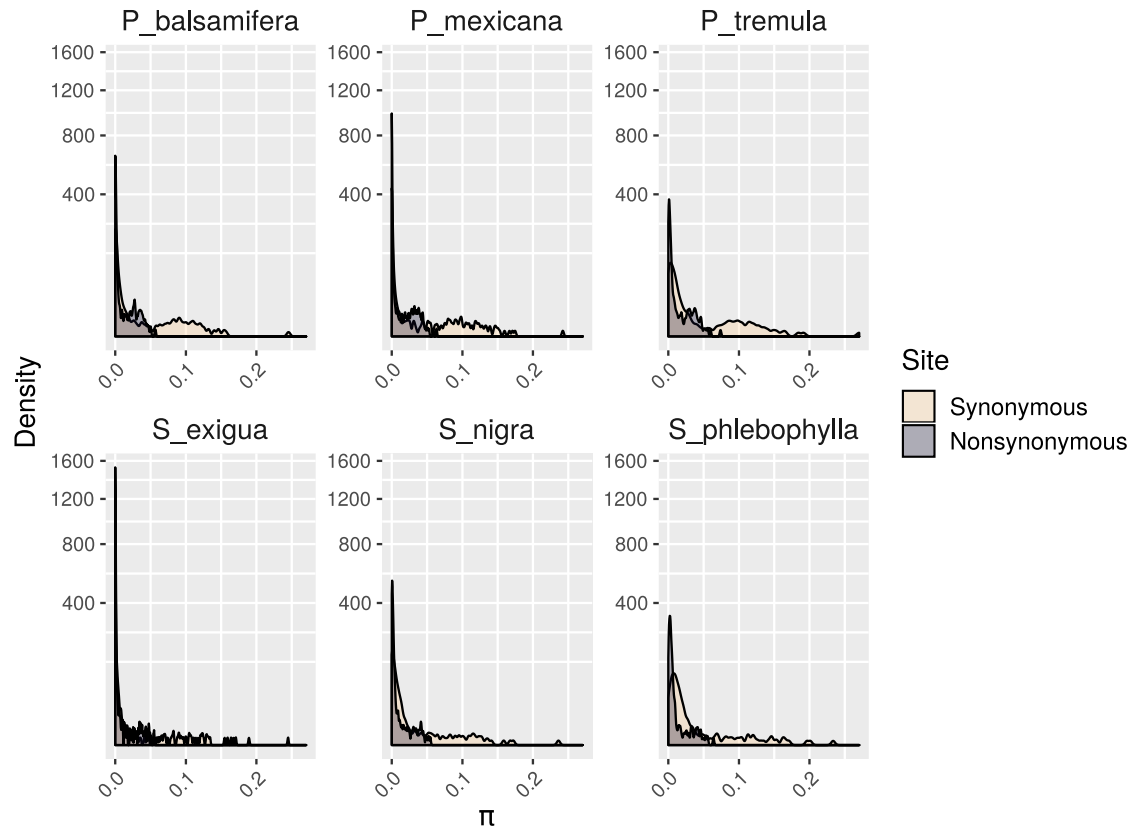
546 327 gene trees support the displayed ASTRAL-III species tree topology. **B)** 44 gene trees and **C)**

547 39 gene trees place one of the *S. phlebophylla* individuals within *S. exigua*.



548

549 **Figure S3.** Species trees estimated for all genes and known paralogs. **A)** Species tree generated
550 by ASTRAL-III for the gene trees. Node values represent bootstrap support from 100 multilocus
551 bootstrap replicates in ASTRAL-III. Branch lengths represent coalescent units. **B)** Cladogram
552 showing the congruence of gene trees for all nodes in the ASTRAL-III species tree. The numbers
553 above each node represent the number of gene trees that support the displayed bipartition, and
554 numbers below the node represent the number of gene trees that support all alternate bipartitions.
555 Purple wedges represent the proportion of gene trees that support the displayed bipartition. Blue
556 wedges represent the proportion of gene trees that support a single alternative bipartition. Green
557 wedges represent the proportion of gene trees that have multiple conflicting bipartitions. Yellow
558 wedges represent the proportion of gene trees that have no supported bipartition. Plotting code
559 and its interpretation were provided by Matt Johnson (for more detail, see:
560 https://github.com/mossmatters/MJPythonNotebooks/blob/master/PhyParts_PieCharts.ipynb)



561

562 **Figure S4.** Distributions of values of nucleotide diversity (Nei's π) within each species at
563 synonymous (yellow) and nonsynonymous (purple) sites.

564